Jet models of X-Ray Flashes(*)

D. Q. LAMB, T. Q. DONAGHY and C. GRAZIANI

Department of Astronomy & Astrophysics, University of Chicago
5640 S. Ellis Ave., Chicago, IL, 60615, USA

Summary. — One third of all HETE-2–localized bursts are X-Ray Flashes (XRFs), a class of events first identified by Heise in which the fluence in the 2–30 keV energy band exceeds that in the 30–400 keV energy band. We summarize recent HETE-2 and other results on the properties of XRFs. These results show that the properties of XRFs, X-ray–rich gamma-ray bursts (GRBs), and GRBs form a continuum, and thus provide evidence that all three kinds of bursts are closely related phenomena. As the most extreme burst population, XRFs provide severe constraints on burst models and unique insights into the structure of GRB jets, the GRB rate, and the nature of Type Ib/Ic supernovae. We briefly mention a number of the physical models that have been proposed to explain XRFs. We then consider two fundamentally different classes of phenomenological jet models: universal jet models, in which it is posited that all GRBs jets are identical and that differences in the observed properties of the bursts are due entirely to differences in the viewing angle; and variable-opening angle jet models, in which it is posited that GRB jets have a distribution of jet opening angles and that differences in the observed properties of the bursts are due to differences in the emissivity and spectra of jets having different opening angles. We consider three shapes for the emissivity as a function of the viewing angle θ_v from the axis of the jet: power law, top hat (or uniform), and Gaussian (or Fisher). We then discuss the effect of relativistic beaming on each of these models. We show that observations can distinguish between these various models.

PACS 98.70.Rz – γ-ray sources; γ-ray bursts.
PACS 01.30.Cc – Conference proceedings.

1. – Introduction

Results from HETE-2 show that the properties of XRFs [14], X-ray–rich GRBs, and GRBs form a continuum in the $[S_E(2-400\,\text{kev}), E_{\text{peak}}^{\text{obs}}]$ plane [32] (see fig. 1, left panel). They also show that the relation between the isotropic-equivalent burst energy E_{iso} and the peak energy E_{peak} of the burst spectrum in νF_ν in the rest frame of the burst found by [1] extends to XRFs and X-ray–rich GRBs(XRRs) [21] (see fig. 1, right panel).
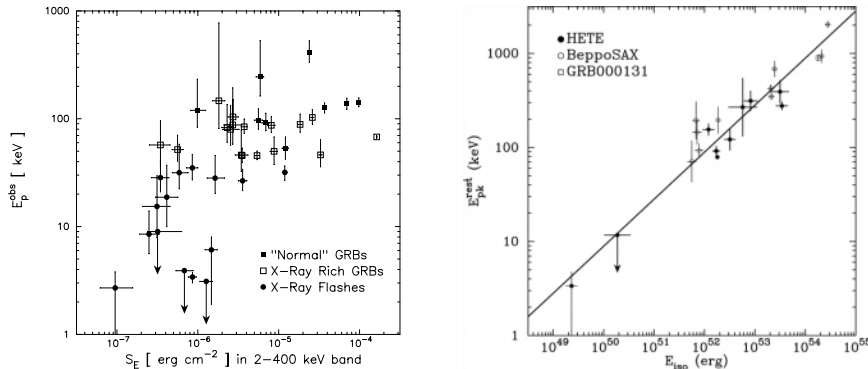
Fig. 1. – Left panel: Distribution of HETE-2 bursts in the $[S(2$–400 keV$), E_{\rm peak}^{\rm obs}]$-plane, showing XRFs (filled circles), X-ray–rich GRBs (open boxes), and GRBs (filled boxes). This figure shows that XRFs and X-ray–rich GRBs comprise about 2/3 of the bursts observed by HETE-2, and that the properties of the three kinds of bursts form a continuum. All error bars are 90% confidence level. From [32]. Right panel: Distribution of HETE-2 and *Beppo*SAX bursts in the $(E_{\rm iso}, E_{\rm peak})$-plane, where $E_{\rm peak}$ is the energy of the peak of the burst νF_ν spectrum in the source frame. The HETE-2 bursts confirm the relation between $E_{\rm iso}$ and $E_{\rm peak}$ found by [1] and extend it by a factor ~ 300 in $E_{\rm iso}$. From [19].

A key feature of the distribution of bursts in these two planes is that the density of bursts is roughly constant along these relations, implying equal numbers of bursts per logarithmic interval in S_E, $E_{\rm peak}^{\rm obs}$, $E_{\rm iso}$ and $E_{\rm peak}$. These results, when combined with earlier results [14, 17], strongly suggest that all three kinds of bursts are closely related phenomena.

However, the nature of XRFs remains largely unknown. Key unanswered questions include the following: Are E_γ (XRFs) $\ll E_\gamma$ (GRBs)? Is the XRF population a direct extension of the GRB and XRR populations? Are XRFs a separate emission component of GRBs? Are XRFs due to different physics than GRBs? Finally, does the burst population extend down to the UV and optical energy bands?

As the most extreme burst population, XRFs provide severe constraints on burst models. In this paper, we review recent theoretical efforts to provide a unified jet picture of XRFs, XRRs, and GRBs, motivated by HETE-2 observations of these three kinds of bursts. We show that observations of XRFs can provide unique insights into the structure of GRB jets, the GRB rate, and the nature of Type Ib/Ic supernovae.

2. – Physical jet models of XRFs

A number of theoretical models have been proposed to explain XRFs. According to [25, 38], X-ray (20–100 keV) photons are produced effectively by the hot cocoon surrounding the GRB jet as it breaks out, and could produce XRF-like events, if viewed well off the axis of the jet. However, it is not clear that such a model would produce roughly equal numbers of XRFs, XRRs, and GRBs, or the nonthermal spectra exhibited by XRFs. The "dirty fireball" model of XRFs posits that baryonic material is entrained in the GRB jet, resulting in a bulk Lorentz factor $\Gamma \ll 300$ [4, 15, 5]. At the opposite extreme, GRB jets in which the bulk Lorentz factor $\Gamma \gg 300$ and the contrast between the bulk Lorentz factors of the colliding relativistic shells are small can also produce XRF-like events [26]. [33-35] have proposed that XRFs are the result of a highly collimated GRB jet outside the opening angle of a jet with sharp edges. In this model,

TABLE I. – *Phenomenological jet models of XRFs considered in this review.*

Jet Profile	Jet Opening Angle	References
Power law	Universal	[10, 12, 20, 23, 27-29, 31, 36]
Power law + Beaming	Universal	[7, 13]
Uniform	Universal	——-
Uniform + Beaming	Universal	[7, 13, 33, 34]
Uniform	Variable	[2, 11, 12, 20, 27, 28, 31]
Uniform + Beaming	Variable	[6, 7, 13, 35]
Gaussian/Fisher	Universal	[3, 8-10, 13, 24, 37]
Gaussian/Fisher + Beaming	Universal	[6, 7, 13]
Gaussian/Fisher	Variable	[8, 9, 13, 31]
Gaussian/Fisher + Beaming	Variable	[6, 7, 13]

the low values of E_{peak} and E_{iso} (and therefore of E_{peak}^{obs} and S_E) seen in XRFs is the result of relativistic beaming. However, it is not clear that such a model can produce roughly equal numbers of XRFs, XRRs, and GRBs, and still satisfy the observed relation between E_{iso} and E_{peak} [1, 19, 21].

3. – Phenomenological jet models of XRFs

In this review, we consider two fundamentally different classes of phenomenological jet models: universal jet models, in which it is posited that all GRBs jets are identical and that differences in the observed properties of the bursts are due entirely to differences in the viewing angle; and variable-opening angle (VOA) jet models, in which it is posited that GRB jets have a distribution of jet opening angles and that differences in the observed properties of the bursts are due to differences in the emissivity and spectra of jets having different jet opening angles. We consider three shapes for the emissivity as a
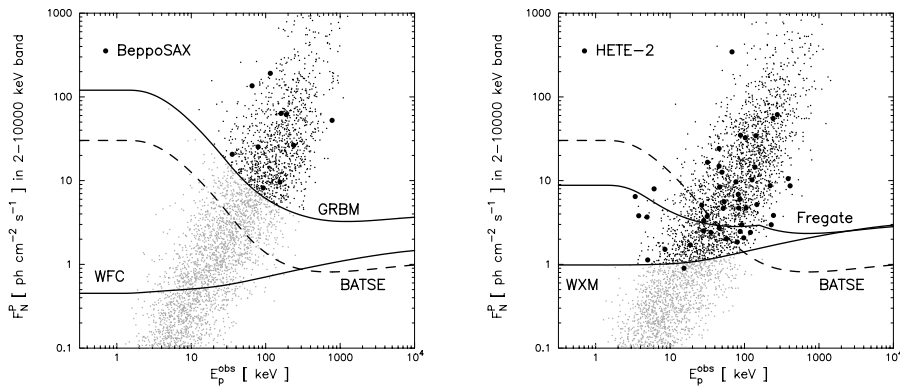

Fig. 2. – Distribution of bursts in the $[E_{peak}^{obs}, F_N^P(2\text{–}10000 \text{ keV})]$-plane detected by *Beppo*SAX (left panel) and by HETE-2 (right panel) compared to the top-hat VOA jet model. Detected bursts are shown in black and non-detected bursts in gray. For each experiment we show the sensitivity thresholds for their respective instruments plotted as solid blue lines. The BATSE threshold is shown in both panels as a dashed blue line. The agreement between the observed and predicted distributions of bursts is good. From [20].
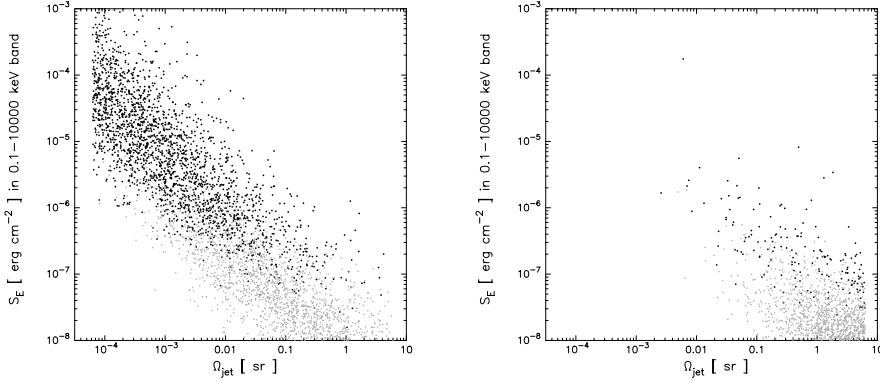
Fig. 3. – Predicted distribution of bursts in the (S_E), (Ω_{jet})-plane in the top-hat VOA jet model (left panel) and in the PL universal jet model (right panel). Bursts detected by the WXM are shown in black and non-detected bursts in gray. The left panel exhibits the constant density of bursts per logarithmic interval in S_E and Ω_{jet} given by the top-hat VOA jet model, while the right panel exhibit the concentration of bursts at $\Omega_{\mathrm{jet}} \equiv \Omega_{\mathrm{view}} \approx 2\pi$, and the resulting preponderance of XRFs relative to GRBs, in the PL universal jet model. From [20].

function of the viewing angle θ_{v} from the axis of the jet: power law, top hat (or uniform), and Gaussian (or Fisher). We also discuss the effect of relativistic beaming on each of these models. Table I lists the various models that we consider.

[10, 12, 20, 23, 27-29, 31, 36] consider a universal jet model for GRBs in which the emissivity is a power law function of the angle relative to the jet axis. In particular, [20] compare the predictions of a variable opening angle (VOA) in which the emissivity is roughly uniform across the head of the jet (see also [2,11,12,27,28,31]) and a universal jet model in which the emissivity is a power law function of the angle relative to the jet axis. They calculate the distributions of the observed properties of GRBs, X-ray–rich GRBs, and XRFs, using Monte Carlo simulations in which they model both the bursts and the observational selection effects introduced by the *Beppo*SAX and HETE-2 instruments (see fig. 2). They show that, while the uniform VOA jet model can account for the observed properties of all three kinds of bursts because of the extra degree of freedom
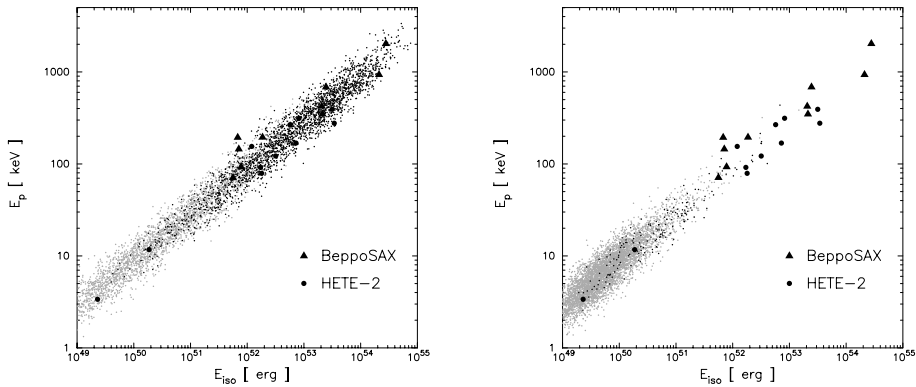

Fig. 4. – Predicted distribution of bursts in the (E_{iso}), (E_{peak})-plane in the top-hat VOA jet model (left panel) and in the PL universal jet model (right panel). Bursts detected by the WXM are shown in black and non-detected bursts in gray. The triangles and circles respectively show the locations of the *Beppo*SAX and HETE-2 bursts with known redshifts. From [20].
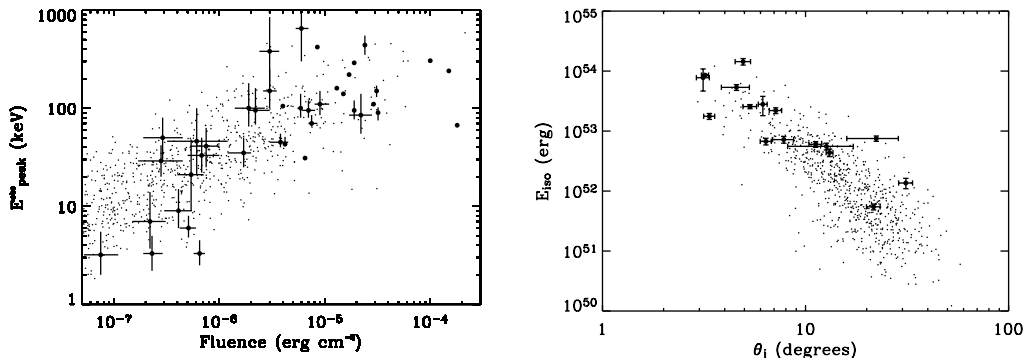
Fig. 5. – Left panel: Comparison of the distribution of simulated bursts in the $(E_{\mathrm{peak}}^{\mathrm{obs}}, S_E)$-plane (small filled circles) for the Gaussian universal jet model and the distribution of observed HETE-2 and *Beppo*SAX bursts (large filled circles with error bars; data from [19]). Right panel: Comparison of the distribution of simulated bursts in the $(E_{\mathrm{iso}}, \theta_{\mathrm{jet}})$-plane (small filled circles) and the observed distribution (large filled circles with error bars; data from [2], using the afterglow jet break time to infer θ_{jet}. Note that the simulated burst distributions are more strongly concentrated at lower values of $E_{\mathrm{peak}}^{\mathrm{obs}}$, S_E, and E_{iso}, and larger values of θ_{jet}, than are the observed burst distributions. From [37].

that having a distribution of jet opening angles gives it, the power law universal jet model cannot account for the observed properties of both XRFs and GRBs (see fig. 3 and 4).

In response to this conclusion, [3,37] proposed a universal Gaussian jet model (see also [10,24,36]). They show that such a model can explain many of the observed properties of XRFs, X-ray–rich GRBs, and GRBs reasonably well (see fig. 5). More recently, [8,9,13] considered a universal jet model in which the emissivity of the jet as a function of viewing angle is a Fisher distribution (such a distribution is the natural extension of the Gaussian distribution to a sphere). They show that this model has the unique property that it produces equal numbers of bursts per logarithmic interval in E_{iso}, and therefore in most burst properties, consistent with the HETE-2 results (see fig. 6, top row). They also show that the Fisher universal jet model produces a broad distribution in the inferred radiated energy E_γ^{inf} (see fig. 6, bottom row). This is true for any non-uniform jet, since in this case $E_\gamma^{\mathrm{inf}} = E_{\mathrm{iso}} \cdot (1 - \cos\theta_{\mathrm{jet}})$, where $\theta_{\mathrm{jet}} = \max(\theta_0, \theta_{\mathrm{v}})$ [3,18], the inferred energy radiated in gamma rays inferred using the prescription of [11], is *not* the same as E_γ^{true}, the true energy radiated in gamma rays. Thus it is no surprise that when [8,9] simulate a Fisher VOA jet model, they find results similar to those for the Fisher universal jet model.

Thus [8,9,13] find that the Fisher universal jet model and the Fisher VOA jet model make very different predictions for the distribution of E_γ^{inf} than does the uniform VOA jet model [20]. Further observations of XRFs can determine this distribution and therefore distinguish between these two models of jet structure.

4. – Relativistic beaming

Relativistic kinematics means that even a "top-hat"-shaped jet will be visible when viewed outside of the jet opening angle, θ_{jet} [16]. Relativistic kinematics also means that E_{iso} and $E_{\mathrm{peak}}^{\mathrm{obs}}$ will be small in such cases. [33,34] used these facts to construct a model in which XRFs are simply classical GRBs viewed at an angle $\theta_{\mathrm{v}} > \theta_{\mathrm{jet}}$. They showed
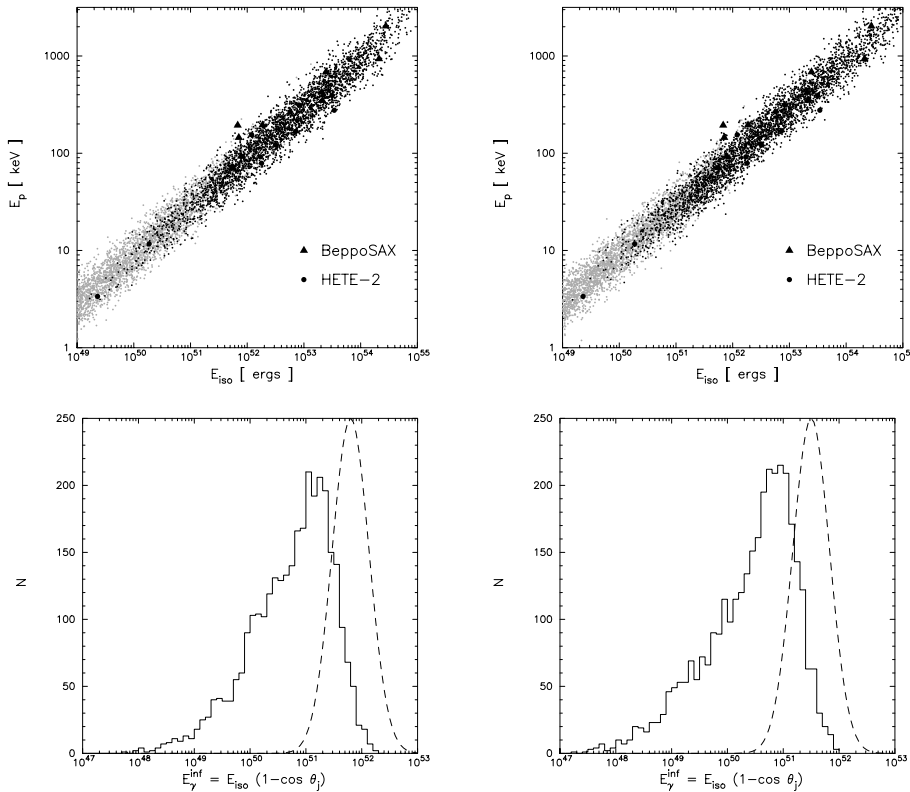
Fig. 6. – Top panels: Predicted distribution of bursts in the (E_{iso}, E_{peak})-plane in the Fisher universal jet model (left) and in the Fisher VOA jet model (right). Bursts detected by the WXM are shown in black and non-detected bursts in gray. Bottom panels: Histograms of E_γ^{inf} values for detected bursts, as compared to the input distribution of E_γ^{true} (dashed curve) for the Fisher universal jet model (left) and the Fisher VOA jet model (right). From [9] (see also [8]).

that such a model could reproduce many of the observed characteristics of XRFs.; in particular, [35] showed that in such a model, the distribution of both on- and off-axis observed bursts was roughly consistent with the $E_{peak} \propto E_{iso}^{1/2}$ relation.

[6, 7, 13] explore further the possibility that the XRFs observed by HETE-2 and *Beppo*SAX are primarily off-axis GRBs. Using and extending the population synthesis techniques described in [20] and [9], they present predictions for the properties of bursts localized by HETE-2. They show that it is difficult to account for the observed properties of XRFs by modeling them solely as ordinary GRBs viewed off-axis. However, since this emission must be observable solely on physical grounds, they seek to understand its relative importance in large burst populations. They therefore revisit the uniform VOA jet model put forward in [20], now including the effects of off-axis beaming. They note that rough constraints on the bulk Γ might be found by considering the fraction of bursts that are not consistent with the $E_{peak} \propto E_{iso}^{1/2}$ relation.

[33-35] work with a fairly detailed model of the burst emission; [6] adopts a simpler model of off-axis beaming in GRB jets. He makes no assumptions about the underlying physics generating the burst; instead, he makes the approximation that the bulk of the
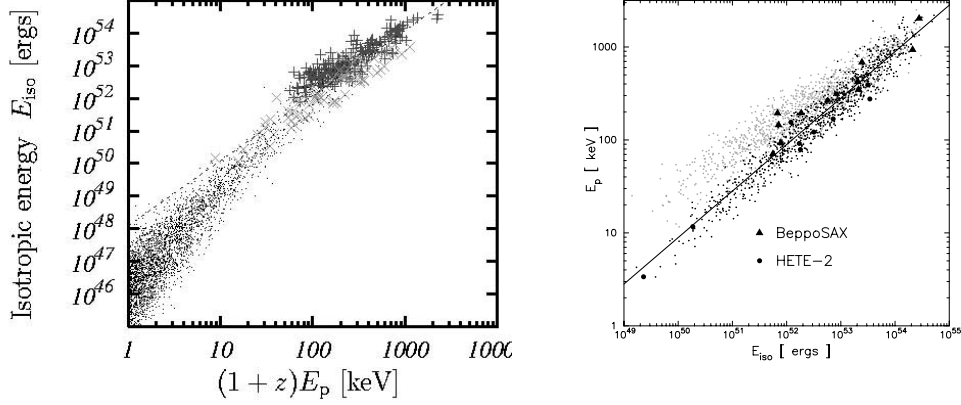
Fig. 7. – Left panel: Simulation of the distribution of bursts in the $(E_{\text{peak}}, E_{\text{iso}})$-plane for a model in which GRBs are due to uniform VOA jets for which $\Gamma = 100$ viewed inside θ_{jet} (crosses) and XRFs are due to the same jets viewed outside θ_{jet} (dots). From [35]. Right panel: The same for a model in which both GRBs and XRFs are due to the variation in the jet opening angle in a uniform VOA jet model with $\Gamma = 300$. From [6].

emission comes directly from the edge of the jet closest to the viewing angle line-of-sight (*i.e.*, he ignores all integrals over the face of the jet and time-of-flight effects). His model therefore focuses on the kinematic transformations of two important burst quantities, E_{iso} and E_{peak}, as a function of viewing angle. A more sophisticated treatment of off-axis is considered in [7, 13].

Relativistic kinematics means that frequencies in the rest frame of the jet will appear Doppler shifted by a factor $\delta^{-1} = \Gamma(1 - \beta \cos \theta)^{-1}$, where β is the velocity of the bulk material and θ is the angle between the direction of motion and the source frame observer. The quantities E_{peak} and E_{iso} then transform as $E_{\text{peak}} \propto E'_{\text{peak}} \delta^{-1}$ and $E_{\text{iso}} \propto E'_{\text{iso}} \delta^{-3}$, where E'_{iso} and E'_{peak} are the values of these quantities at the edge of the jet. For a burst viewed off-axis, these relations imply $E_{\text{peak}} \propto E_{\text{iso}}^{1/3}$. [35] do not consider E_{iso} to be fully bolometric and so derive a slightly different prescription for the off-axis relation.

Figure 7 compares the relative importance of off-axis beaming for two different uniform VOA jet models. The left panel is from [35], who assume $\Gamma = 100$ and draw θ_{jet} values from a power law distribution given by $f_0 \, \mathrm{d}\,\theta_{\text{jet}} \propto \theta_{\text{jet}}^{-2} \, \mathrm{d}\,\theta_{\text{jet}}$, defined from 0.3 to 0.03 rad. This model attempts to explain classical GRBs in terms of the variation of jet opening angles, while XRFs are interpreted as bursts viewed from outside but close to their jet opening angle. [6] attempts to explain both GRBs and XRFs by a distribution of jet opening angles, following the results presented in [20]. He adds off-axis beaming to this picture. The right panel shows the results for $\Gamma = 300$.

[6] finds that the relative importance of off-axis events increases for models which have very small opening angles. This is mainly due to the fact that narrower jets with a constant E_{γ} will have larger E_{iso} values, and therefore such bursts viewed off-axis will also be brighter. However, fig. 7 (right panel) shows that the HETE-2 XRFs are not easily explained as classical GRBs viewed off-axis. The two XRFs with known redshifts lie along the $E_{\text{peak}} \propto E_{\text{iso}}^{1/2}$ relation, and furthermore the larger sample of HETE-2 XRFs without known redshifts do not fall in the region of the $(E_{\text{peak}}^{\text{obs}}, S_{\text{E}})$-plane expected for this model: they lie at lower, rather than higher, $E_{\text{peak}}^{\text{obs}}$ values for a given S_{E}. Even given

the model of the off-axis emission in [35], these HETE-2 XRFs are difficult to explain.

[6] also considers models that generate XRFs that obey the $E_{\text{peak}} \propto E_{\text{iso}}^{1/2}$ relation by extending the range of possible jet opening-angles to cover five orders of magnitude (see [20] for details and discussion). Hence, XRFs that obey the $E_{\text{peak}} \propto E_{\text{iso}}^{1/2}$ relation are bursts that are seen on-axis, but have larger jet opening angles. Nonetheless, these models generate a significant population of off-axis events, although increasing Γ reduces the fraction of off-axis bursts in the observed sample.

REFERENCES

[1] AMATI, L. *et al.*, *A&A*, **390** (2002) 81.
[2] BLOOM, J., FRAIL, D. A. and KULKARNI, S. R., *ApJ*, **588** (2003) 945.
[3] DAI, X. and ZHANG, B., *ApJ*, **620** (2005) 355.
[4] DERMER, C. D., CHIANG, J. and BÖTTCHER, M., *ApJ*, **513** (1999) 656.
[5] DERMER, C. D. and MITMAN, K. E.,, in *Gamma-Ray Bursts in the Afterglow Era*, edited by M. FEROCI, F. FRONTERA, N. MASETTI and L. PIRO, *ASP Conf. Ser.*, **312** (ASP, San Francisco) 2003, p. 301.
[6] DONAGHY, T. Q., these proceedings (2005).
[7] DONAGHY, T. Q., submitted to *ApJ*, 2005.
[8] DONAGHY, T. Q., LAMB, D. Q. and GRAZIANI, C., these proceedings (2005).
[9] DONAGHY, T. Q., LAMB, D. Q. and GRAZIANI, C., submitted to *ApJ*, 2005.
[10] FIRMANI, C. *et al.*, *ApJ*, **608** (2004) 95.
[11] FRAIL, D. *et al.*, *ApJ*, **562** (2001) L55.
[12] GRANOT, J. and KUMAR, P., *MNRAS*, **341** (2003) 263.
[13] GRAZIANI, C., LAMB, D. Q. and DONAGHY, T. Q., submitted to *ApJ*, 2005.
[14] HEISE, J. *et al.*, in Proc. *2nd Rome Workshop: Gamma-Ray Bursts in the Afterglow Era*, edited by E. COSTA, F. FRONTERA, J. HJORTH (Springer-Verlag, Berlin) 2000, p. 16.
[15] HUANG, Y. F., DAI, Z. G. and LU, T., *MNRAS*, **332** (2002) 735.
[16] IOKA K. and NAKAMURA T., *ApJ*, **554** (2001) L163.
[17] KIPPEN, R. M., et al. in Proc. *Gamma-Ray Burst and* and *Afterglow Astronomy*, edited by G. R. RICKER and R. K. VANDERSPEK, *AIP Conf. Proc.*, **662** (AIP, New York) 2002, p. 244.
[18] KUMAR, P. and GRANOT, J., *ApJ*, **591** (2003) 1075.
[19] LAMB, D. *et al.*, *New Astronomy Rev*, **48** (2004) 423.
[20] LAMB, D. Q., DONAGHY, T. Q. and GRAZIANI, C., *ApJ*, **620** (2005) 355.
[21] LAMB, D. Q. *et al.*, *ApJ*, submitted, 2005.
[22] LIANG, E. W., DAI, Z. G. and WU, X. F., *ApJ*, **606** (2004) L29.
[23] LIANG, E. W., WU, X. F. and DAI, Z. G., *ApJ*, **611** (2004) 1033.
[24] LLOYD-RONNING, N. M., DAI, X. and ZHANG, B., *ApJ*, **592** (2003) 1002.
[25] MÉSZÁROS, P., RAMIREZ-RUIZ, E., REES, M. J. and ZHANG, B., *ApJ*, **578** (2002) 812.
[26] MOCHKOVITCH, R., DAIGNE, F., BARRAUD, C. and ATTEIA, J. L., in *Gamma-Ray Bursts in the Afterglow Era, ASP Conf. Ser.*, **312** (ASP, San Francisco) 2003, p. 381.
[27] NAKAR, E., GRANOT, J. and GUETTA, D., *ApJ*, **601** (2004) 119.
[28] NORRIS, J. P., *ApJ*, **571** (2002) 876.
[29] PERNA, R., SARI, S. and FRAIL, D., *ApJ*, **594** (2003) 379.
[30] RAMIREZ-RUIZ, E. and LLOYD-RONNING, N., *New Astronomy*, **7** (2002) 197.
[31] ROSSI, E. M. *et al.*, *MNRAS*, **354** (2004) 81.
[32] SAKAMOTO, T. *et al.*, *ApJ*, submitted, 2004 (astro-ph/0409128).
[33] YAMAZAKI, R., IOKA K. and NAKAMURA T., *ApJ*, **571** (2002) L31.
[34] YAMAZAKI, R., IOKA K. and NAKAMURA T., *ApJ*, **593** (2003) 941.
[35] YAMAZAKI, R., IOKA K. and NAKAMURA T., *ApJ*, **606** (2004) L33.
[36] ZHANG, B. and MÉSZÁROS, P., *ApJ*, **571** (2002) 876.
[37] ZHANG, B., DAI, X., LLOYD-RONNING, N. M. and MÉSZÁROS, P., *ApJ*, **601** (2004) L119.
[38] ZHANG, W., WOOSLEY, S. E. and HEGER, A., *ApJ*, **608** (2004) 365.